

Ultra small angle neutron scattering study of the nanometer to micrometer structure of porous Vycor

Man-Ho Kim^{a,b,*}, Charles J. Glinka^a

^a NIST Center for Neutron Research, National Institute of Standards and Technology, Gaithersburg, MD 20899-8562, United States

^b Department of Materials Science and Engineering, University of Maryland, College Park, MD 20742-2115, United States

Received 28 October 2005; received in revised form 13 December 2005; accepted 15 December 2005

Available online 7 February 2006

Abstract

Ultra small angle neutron scattering (USANS) and SANS measurements, covering length scales from nanometers to micrometers, were made to investigate the structure of monolithic porous Vycor.¹ USANS from dry Vycor showed strong very low angle scattering below scattering vector $q = 0.001 \text{ \AA}^{-1}$ while SANS showed the typical inter-pore correlation peak at $q = 0.023 \text{ \AA}^{-1}$. When the sample was saturated with a 60/40 D₂O/H₂O vol/vol mixture with a neutron scattering density matched to silica framework, the inter-pore correlation peak disappeared as expected confirming that all the nanopores are interconnected. However, the very low angle scattering related to micrometer structure remained prominent even in the contrast matched liquid. The origin of the residual low q scattering is discussed.

© 2005 Elsevier Inc. All rights reserved.

Keywords: Ultra small neutron scattering (USANS); SANS; Contrast matching; Porous Vycor glass; Simulated 2D TEM

1. Introduction

Porous Vycor (7930) glass (trade name of Corning) has a narrow pore size distribution and a large internal surface area of approximately 150–200 m²/g [1]. This much studied material has various applications in chemical separation (membrane and filter) and catalysis [2]. Numerous experiments have been performed on the porous glass to understand its pore structure [3,4], physical phenomena in a confined environment [5–8], and sorption/desorption behavior [9,10]. Simultaneously, various simulations have

been performed to understand hysteresis in adsorption [11–13] and to model the structure of Vycor [11,14,15].

Most of small-angle scattering studies of Vycor have focused on a limited region of the scattering vector, $q (= 4\pi \sin(\theta/2)/\lambda) > 0.005 \text{ \AA}^{-1}$ that corresponds to the scale of $2\pi/q < 1300 \text{ \AA}$, where θ and λ are the scattering angle and the radiation wavelength, respectively. The emphasis of these studies has been to understand the structure related to the prominent peak at $q = 0.023 \text{ \AA}^{-1}$ and to study the surface morphology [16]. The peak is understood to originate from the well defined pore spacing in the SiO₂ matrix. There have been experiments showing an indication of an upturn in the low q -region below $q = 0.005 \text{ \AA}^{-1}$ in SAXS [3,10] and SANS [4] as well as in theoretical calculations [14,15]. This suspected low angle up-turn, however, has not been fully explored or understood. The low angle up-turn observed in SAXS on a powdered Vycor sample was attributed to scattering from the powder grains [16]. It has been reported that the low angle up-turn in SANS was not observed in a monolithic piece of Vycor [16] but

* Corresponding author. Tel.: +1 301 975 6469.

E-mail address: man-ho.kim@nist.gov (M.-H. Kim).

¹ Certain commercial equipment, instruments, or materials are identified in this paper to foster understanding. Such identification does not imply recommendation or endorsement by the National Institute of Standards and Technology, nor does it imply that the materials or equipment identified are necessarily the best available for the purpose.

the scattering profile was not provided. Based on the literature surveyed, there is no clear evidence whether or not a low angle up-turn is an intrinsic feature of the structure of Vycor.

The purpose of this study is to confirm whether the up-turn at low- q can be observed in monolithic Vycor samples, and to determine whether the low angle up-turn is related to the structure that gives rise to the main peak near $q = 0.023 \text{ \AA}^{-1}$. The high flux USANS facility at NIST-NCNR [17,18] enables measurements to $q \sim 3.0 \times 10^{-5} \text{ \AA}^{-1}$, roughly two decades lower than the low q limit of previous small angle scattering studies of Vycor.

The NCNR USANS instrument is a Bonse–Hart-type instrument which uses a pair of triple-bounce channel-cut perfect Silicon crystals as monochromator and analyzer to give high angular resolution in the scattering plane, albeit with poor resolution in the perpendicular (vertical) direction. The layout of the USANS instrument is shown in Fig. 1.

The so-called slit-smear cross section measured in USANS, $((d\Sigma/d\Omega)(q))_{\text{usans}}^s$ (where the superscript s stands for smearing), is related to the cross section, $(d\Sigma/d\Omega)(q)$, measured with pinhole collimation by the expression:

$$\left(\frac{d\Sigma}{d\Omega}(q)\right)_{\text{usans}}^s = \frac{1}{\Delta q_v} \int_0^{\Delta q_v} \frac{d\Sigma}{d\Omega}(\sqrt{q^2 + u^2}) du, \quad (1)$$

where the full-width at half-maximum (FWHM) of the vertical q -resolution, Δq_v , has been determined to be 0.117 \AA^{-1} , when the USANS cross-section is desmeared numerically by inverting Eq. (1), the slope of the measured q -dependence of the scattering is decreased by 1.

The neutron scattering contrast of a porous material can be varied by filling the pores with hydrogenated (H) and deuterated (D) solvent mixtures because the total scattering

cross section, $(d\Sigma/d\Omega)(q)$, depends on the SLD difference between the matrix and pores:

$$\frac{d\Sigma}{d\Omega}(q) \propto c\phi_{\text{matrix}}\phi_{\text{pore}}(\langle \text{SLD}_{\text{matrix}} \rangle - \text{SLD}_{\text{pore}})^2 \cdot K(q), \quad (2)$$

where, c is an instrument constant, ϕ is volume fraction, $\langle \rangle$ is average, and SLD is defined as $\text{SLD} = (\sum_i^n b_i)/V$ for neutrons. b_i is the bound coherent scattering length of atomic species i , and $1/V = \rho N_A/M_w$ is a number density ($\#/cm^3$) expressed in terms of the bulk density (ρ , g/cm^3), Avogadro's number (N_A), and molecular weight (M_w) of a substance. $K(q)$ describes a shape and/or structure factor, which depends on the orientation, polydispersity, and volume fraction of the scattering objects. If there is any relation between the pore interference peak and the low angle scattering, or there are macro size pores, it is expected that both the pore correlation peak at $q = 0.023 \text{ \AA}^{-1}$ and the low q up-turn in the scattering should disappear (i.e., $\frac{d\Sigma}{d\Omega}(q) = 0$) since $\langle \text{SLD}_{\text{matrix}} \rangle = \text{SLD}_{\text{pore}} = \text{SLD}_{\text{mixture}}$, when a contrast matched D_2O/H_2O mixture fills all of the randomly interconnected pores as shown in Fig. 2.

2. Experimental

A Vycor disk, 0.9 mm thick and 20 mm in diameter, was cleaned in a 30 mass% hydrogen peroxide solution in water at $100 \text{ }^\circ\text{C}$ for 3 h, rinsed with deionized water several times, and kept in deionized water for two days prior to the experiment. The clean wet Vycor was then dried under vacuum at about $100 \text{ }^\circ\text{C}$ by raising temperature (approximately $10 \text{ }^\circ\text{C/h}$) slowly to avoid cracks due to heterogeneous thermal expansion of water in the pores. The cleaned dry Vycor was colorless and translucent. The USANS and SANS

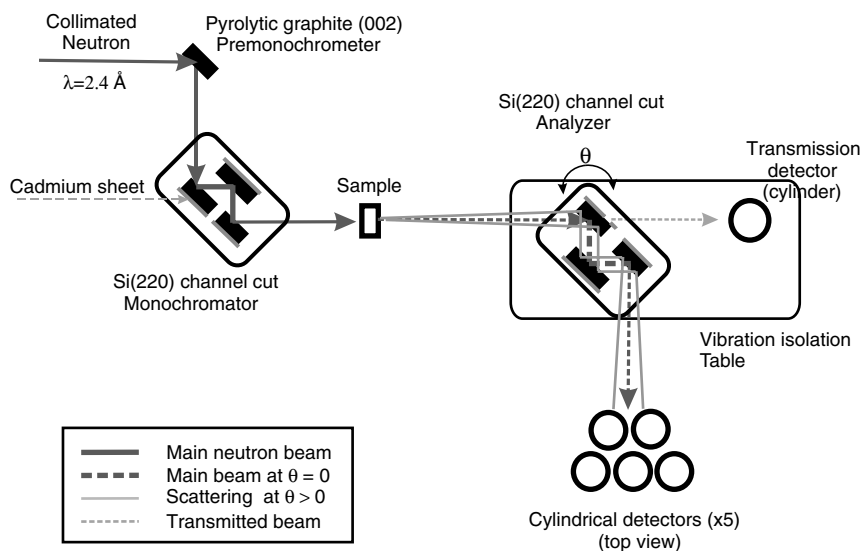


Fig. 1. Schematic of the NCNR's Bose–Hart-type ultra small neutron scattering instrument (USANS). When the two triple-bounce crystals are aligned ($\theta = 0$), the incident beam is totally reflected into the main detector bank. When the analyzer crystal is rotated by an angle θ , only the small-angle scattering corresponding to the same angle θ is reflected.

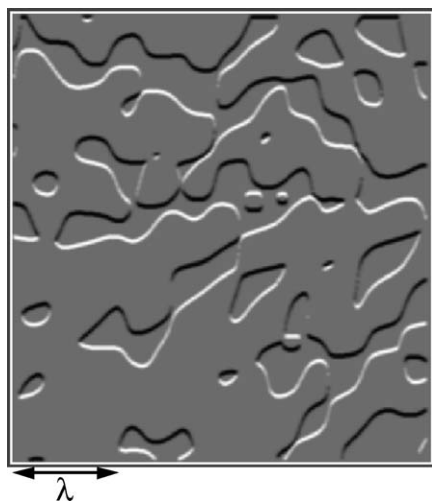


Fig. 2. Simulated 2D TEM image of dry Vycor structure based on the random standing wave model introduced by Cahn [26] and refined by Berk [14,15]. The simulation was done for a pore volume fraction of, $\phi_v \approx 0.266$, an average wavelength, $\lambda (=2\pi/q_{\text{peak}}) = 273 \text{ \AA}$, for the standing waves and a wavelength distribution of 0.0015. The estimated average pore size is approximately 73 \AA from $\lambda \cdot \phi_v$. Ref. [1,5] show an actual TEM image.

measurements on the dry Vycor were measured under ambient conditions. The wet Vycor for contrast variation experiment was prepared as follows. For SANS, the dry Vycor was first placed in the evacuated in situ sorption cell (path length: 1 mm) [19] for removing air trapped in the pores and for further drying. The various $\text{D}_2\text{O}/\text{H}_2\text{O}$ vol/vol mixtures were directly injected into the evacuated cell to fill the evacuated pores and SANS measurements were performed in situ. For the USANS measurements, samples wet in the sorption cell were transferred to standard 2 mm path length closed cells for experimental convenience. Additional liquid was added to fill the cell volume completely. The cell was centrifuged to remove bubbles in the bulk liquid and the sample. The $\text{D}_2\text{O}/\text{H}_2\text{O}$ mixtures used for contrast variation were 60/40, 62/38, pure H_2O , and pure D_2O for SANS and an additional 77/33 for USANS.

The measured scattering was converted to the total cross-section (i.e., absolute units, cm^{-1}) by subtracting the scattering from an empty cell and ambient background, and by normalizing with the sample transmission and thickness. In order to confirm that multiple scattering was insignificant, the sample transmission was measured in two ways. One is to measure the ratio ($T_{\text{rock}} = I(0)_{\text{sample}}/I(0)_{\text{empty}}$) of the rocking curve peak intensity (count rate) at $q = 0$ with the main detector bank. Then, with the analyzer crystal turned to a relatively large angle (a few degrees), the ratio of the counts recorded in the transmission detector (see Fig. 1) with and without the sample provides another measure of the sample transmission, denoted $T(\text{wide})$. The transmission detector captures all of the small-angle scattering from the sample and thus $T(\text{wide}) > T(\text{rock})$. However, if they are not very different only a small fraction of

the beam has undergone small-angle scattering. In the present case, the two transmissions were more than 90%, which means that there was negligible multiple scattering [20,21].

3. Results and discussion

3.1. Dry Vycor

Fig. 3 shows the measured USANS scattering, $((d\Sigma/d\Omega)(q))_{\text{USANS}}$ (red circles) of dry Vycor in the q range from 3×10^{-5} to $\sim 3.0 \times 10^{-2} \text{ \AA}^{-1}$ and SANS (closed black circles) in the q range from 1×10^{-3} to $\sim 4.0 \times 10^{-1} \text{ \AA}^{-1}$. The Vycor main peak ($q = 0.023 \text{ \AA}^{-1}$) appears as a weak hump in the measured USANS due to slit-smearing effect. In SANS, the main peak (i.e., pore correlation peak) appears as a strong peak due to the pinhole collimation. The USANS profile (i.e., smeared cross-section) shows a strong low angle up-turn with a slope of -2.6 ± 0.2 . The slope is an averaged value of two measurements. Note that a slope of -2.6 in USANS corresponds to -3.6 in SANS by Eq. (1). (The error reported here corresponds the largest possible one and was derived by considering the different q regions of the two measurements.)

The reliability of the procedure for putting the slit-smear USANS cross-section $((d\Sigma/d\Omega)(q))_{\text{USANS}}$ on an absolute scale was confirmed by comparing with the SANS cross-section, $((d\Sigma/d\Omega)(q))_{\text{SANS}}$, obtained from the 2 dimensional detector and pin-hole collimation. Due to the differences in detector geometry between USANS and SANS instrument, the absolute intensities between the two can be compared by either smearing $((d\Sigma/d\Omega)(q))_{\text{SANS}}$ or

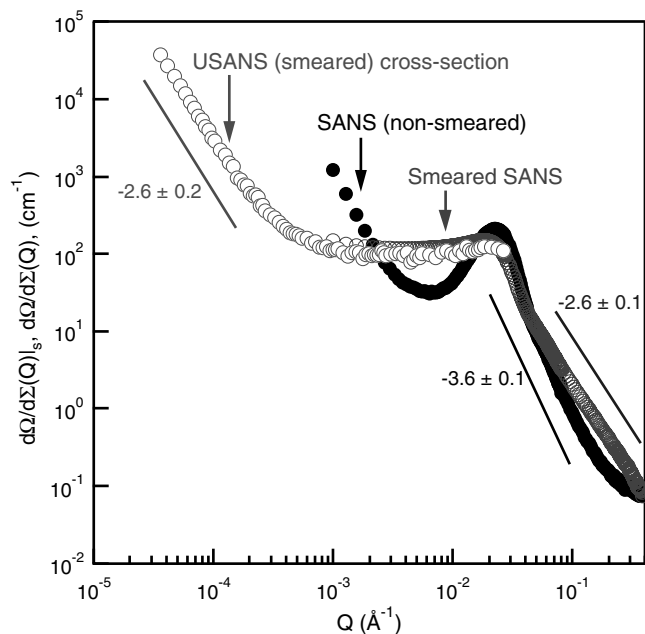


Fig. 3. Measured USANS (red open) and SANS (black closed) profiles of dry Vycor. Slit-smearing the SANS data (blue open) allows direct comparison with the slit-smear USANS data. (For interpretation of the references to color in this figure legend, the reader is referred to the web version of this article.)

desmearing $((d\Sigma/d\Omega)(q))_{\text{usans}}^{\text{ds}}$. The result by the latter method will be shown in a later section. Here, the result by the former method is shown (blue circle in Fig. 3). When the measured $((d\Sigma/d\Omega)(q))_{\text{sans}}$ is smeared numerically, the profile of $((d\Sigma/d\Omega)(q))_{\text{sans}}^{\text{ds}}$ agrees well with the measured $((d\Sigma/d\Omega)(q))_{\text{usans}}^{\text{ds}}$ on an absolute scale.

The smeared SANS data show several characteristic features of smearing. The well-defined strong pore correlation peak ($q = 0.023 \text{ \AA}^{-1}$) and the low angle up-turn in $(d\Sigma/d\Omega)(q)_{\text{sans}}$ become almost flat and the slope of -3.6 on the high- q side of the main peak becomes -2.6 as expected from the analytical solution of Eq. (1) in the case of a power law. In spite of the slit smearing effect in USANS, the scattering does show a strong very low angle upturn below $q = 0.001 \text{ \AA}^{-1}$ and continues to rise at the lowest accessible q . This demonstrates that the weak low- q upturn observed in several SAS measurements [4,10] does originate from the dry Vycor structure. In other words, the very low angle scattering exists even in a continuous macroscopic piece of Vycor, contrary to the conclusion of Höhr et al. [16]. Höhr et al. reported that no low angle up-turn was observed in a monolithic piece of Vycor porous glass, although they did show a low q upturn from a powdered sample in the range from $q = (0.003 \text{ to } 0.01) \text{ \AA}^{-1}$ as expected. Unfortunately, it is not possible to know the low q resolution of their SANS measurement since no SANS intensity profile for a monolithic piece was provided.

The power law index $n \cong 3.6$ of the USANS scattering, $((d\Sigma/d\Omega)(q))_{\text{usans}}^{\text{ds}} = ((d\Sigma/d\Omega)(0))_{\text{usans}}^{\text{ds}} q^{-n}$, (the superscript ds means desmeared), of dry Vycor in the very low q region (below $q = 10^{-3} \text{ \AA}^{-1}$) suggests that Vycor has fractal surfaces with a dimensionality of $D = 2.4 \pm 0.2$. The fractal dimensionality, D , is defined as $n = 6 - D$ in 3D object.

The power law index in the very low angle (USANS) range is identical with that in the high q region (SANS) within experimental error, suggesting a fractal structure in both the nanometer and micrometer scale. The power law at high q is known to depend on the amount of water in Vycor [22,23]. The value of $n = -3.6$ is consistent with Benham et al.'s [22] value for dry Vycor rather than Schaefer et al.'s [3] ($n = -4$). The latter has been challenged by Benham et al. due to the existence of moisture in the sample.

A shoulder around $q = 0.06 \text{ \AA}^{-1}$ in the SANS of the dry Vycor in Fig. 5 was also seen in SAXS [10]. It is not known whether this weak hump represents an independent structure or a higher order peak of the primary pore structure.

The question arises as to the origin of the very low q scattering, which indicates the presence of inhomogeneities larger than around 10 \mu m . The measurements described in the next section were undertaken to address this question.

3.2. Wet Vycor

If the large-scale structure that gives rise to the low angle up-turn in the scattering is due to accessible porosity, it is

expected to disappear when the pores are filled with a neutron null contrast liquid, i.e., SLD_{pore} is replaced with the liquid with $\langle \text{SLD}_{\text{matrix}} \rangle = \text{SLD}_{\text{liquid}}$ in Eq. (2). The composition of the matrix is known to consist of 97 mass% SiO_2 and 3 mass% B_2O_3 [1]. Because slightly different SLD matching points, in the range of $3.35\text{--}3.80 \times 10^{10} \text{ cm}^{-2}$ [24–26], have been reported for Vycor, we re-measured the SLD matching point for our samples.

Fig. 4(a) shows that the $((d\Sigma/d\Omega)(q))_{\text{sans}}$ at $q = 0.023 \text{ \AA}^{-1}$ of the Vycor sample wet with 60/40 $\text{D}_2\text{O}/\text{H}_2\text{O}$ liquid is reduced by a factor of $\sim 10^3$ compared to that of the dry sample, although reproducibility is not perfect. The inter-pore correlation peak did not disappear com-

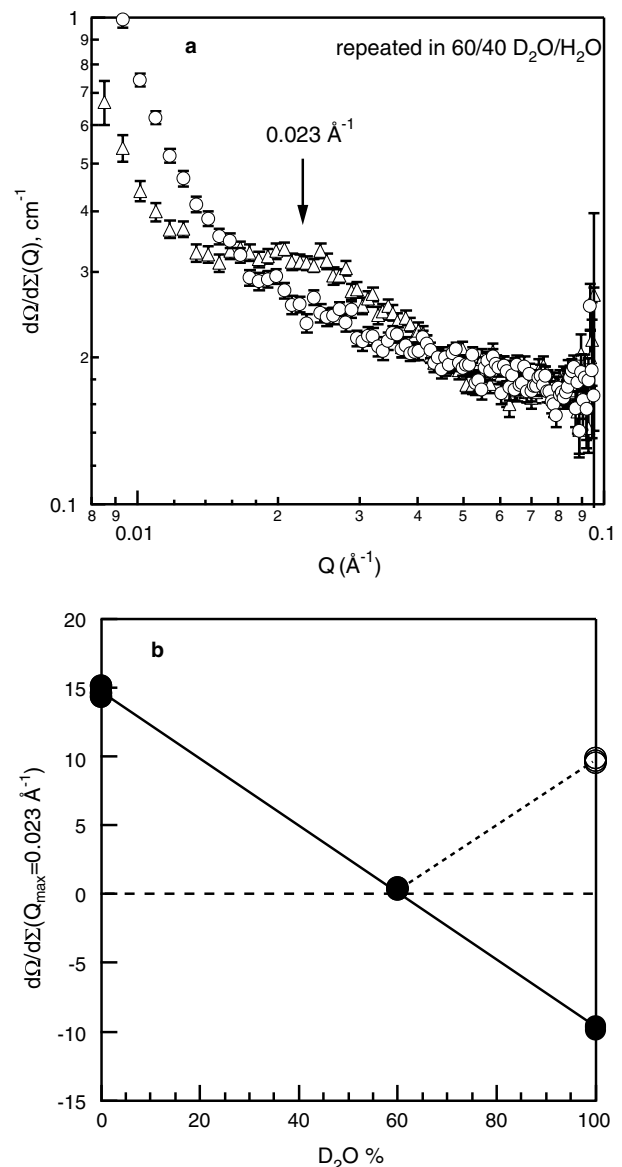


Fig. 4. (a) SANS profiles of Vycor wetted by injecting a 60% $\text{D}_2\text{O}/40\%$ H_2O /mixture under vacuum. The experiment was done twice (open circle and triangle) to check reproducibility; (b) the contrast matching plot. Open and closed circles are the positive and negative square roots of the measured intensity, respectively.

pletely in one measurement but disappeared in another measurement.

The contrast match point was determined from a plot of $\sqrt{(d\Omega/d\Sigma)(q_{\max})}$ vs. D_2O vol% (Fig. 4(b)), where $q_{\max} = 0.023 \text{ \AA}^{-1}$. $\sqrt{(d\Omega/d\Sigma)(q_{\max})}$ is used instead of $\sqrt{(d\Omega/d\Sigma)(0)}$ since the origin of the residual low angle up-turn is not known. The $\sqrt{(d\Omega/d\Sigma)(q_{\max})}$ at 60/40 D_2O/H_2O is nearly zero, corresponding to $SLD = 3.574 \times 10^{10} \text{ cm}^{-2}$. Fig. 4(b) also shows that $\sqrt{(d\Omega/d\Sigma)(q_{\max})}$ at 60/40 D_2O/H_2O lies on a straight line when $\sqrt{(d\Omega/d\Sigma)(q_{\max})}$ is plotted versus the percentage of D_2O in the series of mixtures used, further demonstrating the contrast matching (CM) mixture is 60/40 D_2O/H_2O . (The calculated CM with a bulk density 2.18 g/cm^3 for Vycor, SLD of $-5.6 \times 10^9 \text{ cm}^{-2}$ for H_2O , and $6.33 \times 10^{10} \text{ cm}^{-2}$ for D_2O is 59/41 D_2O/H_2O and the corresponding SLD is $3.4976 \times 10^{10} \text{ cm}^{-2}$ assuming an ideal solution.) The 60/40 mixture will be called the contrast matching (CM) point or contrast matched (CM) mixture to the Vycor main peak in this study. This mixture is used for the USANS measurements to investigate whether the strong very low angle scattering observed in the dry Vycor shows the same intensity reduction as the pore correlation peak.

Combined USANS and SANS scattering profiles for wet Vycor in the CM liquid and dry Vycor are shown in Fig. 5. This time, $((d\Sigma/d\Omega)(q))_{\text{USANS}}^s$ was desmeared to be compared with the measured $((d\Sigma/d\Omega)(q))_{\text{SANS}}$. Again, the desmeared USANS, $((d\Sigma/d\Omega)(q))_{\text{USANS}}^{\text{ds}}$, agrees well with

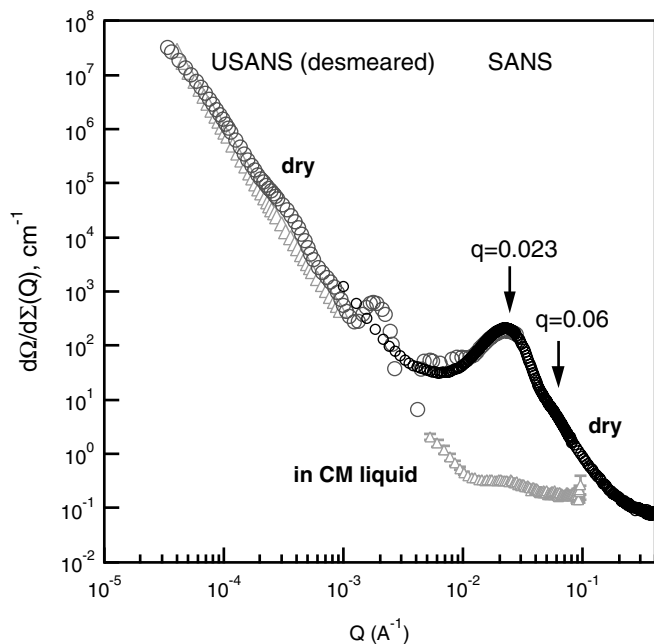


Fig. 5. Combined plot of USANS and SANS for Vycor (triangle) wetted in the CM liquid and dry Vycor (circle). There is a gap in the data for the CM liquid because the USANS signal merged with background above $Q = 0.001 \text{ \AA}^{-1}$ and the SANS measurements did not extend to low enough $Q (\text{Å}^{-1})$ to overlap with the USANS data. (For interpretation of the references to color in this figure legend, the reader is referred to the web version of this article.)

$((d\Sigma/d\Omega)(q))_{\text{USANS}}^s$, although there is some artificial oscillation in $((d\Sigma/d\Omega)(q))_{\text{USANS}}^{\text{ds}}$ around $q = 10^{-3}$ to 6×10^{-3} demonstrating the limitations of the desmearing procedure. The barely observable main peak in $((d\Sigma/d\Omega)(q))_{\text{USANS}}^s$ (see Fig. 3 (red circle)) becomes prominent in $((d\Sigma/d\Omega)(q))_{\text{USANS}}^{\text{ds}}$ (Fig. 5 blue circle). Fig. 5 shows that the low angle upturn (green triangle) is hardly affected by the CM mixture while $((d\Sigma/d\Omega)(q))_{\text{USANS}}^s$ at $q = 0.023 \text{ \AA}^{-1}$ almost disappears as shown in Fig. 4(a).

The $((d\Sigma/d\Omega)(q))_{\text{USANS}}^s$ for several H_2O/D_2O mixtures is shown in Fig. 6(a) along with the dry Vycor data. A contrast variation plot constructed from these data is shown

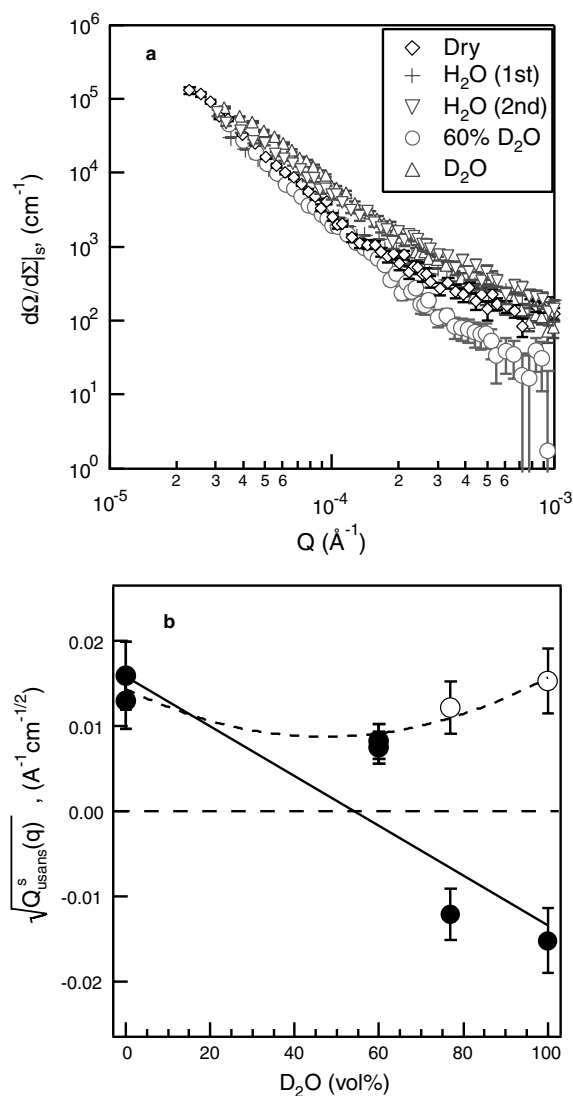


Fig. 6. (a) Some selected USANS (smeared) cross-sections (unit cm^{-1}) of Vycor dry, in pure H_2O , pure D_2O , and 60/40 D_2O/H_2O mixture. (b) USANS contrast matching plot (invariant vs. D_2O vol%). The invariant was calculated using the measured USANS $((d\Sigma/d\Omega)(q))_{\text{USANS}}^s$ in the q range of $q = 3 \times 10^{-5}$ to 10^{-3} \AA^{-1} . D_2O/H_2O mixture ratios are pure D_2O , 77/33, 62/38, 60/40, and pure H_2O . USANS was measured twice at each ratio. Open and closed circles are the positive and negative square roots of the measured intensity, respectively. Dashed line is for a guide of eye and solid line is a linear fit of closed symbols (see text for details).

Table 1
Contrast $(\Delta \text{SLD})^2$, between various matrix compositions and $\text{D}_2\text{O}/\text{H}_2\text{O}$ mixtures

	Density ^b (g/cm ³)	SLD (cm ⁻²)	$(\Delta \text{SLD})^2$ (cm ⁻⁴)			
CM(60/40 $\text{D}_2\text{O}/\text{H}_2\text{O}$)		3.57E+10				
(77/23 $\text{D}_2\text{O}/\text{H}_2\text{O}$)		4.75E+10				
SiO_2 (amorphous)	2.200	3.47E+10	CM– SiO_2	77D/23H– SiO_2		
			1.08E+18	1.63E+20		
Amorphous matrix ^a		3.50E+10	CM–matrix	77D/23H–matrix		matrix– SiO_2
			5.84E+17	1.56E+20		7.62E+16
B_2O_3 (amorphous)	1.812	4.39E+10	CM– B_2O_3 (a)	77D/23H– B_2O_3 (a)	B_2O_3 (a)– SiO_2	matrix– B_2O_3 (a)
			6.66E+19	1.26E+19	8.46E+19	7.96E+19
B_2O_3 (crystal)	2.460	5.96E+10	CM– B_2O_3 (c)	77D/23H– B_2O_3 (c)	B_2O_3 (c)– SiO_2	matrix– B_2O_3 (c)
			5.69E+20	1.48E+20	6.20E+20	6.06E+20

^a Matrix chemical composition consists of SiO_2 97% and B_2O_3 (3%). Other components, Na_2O and $\text{Al}_2\text{O}_3+\text{ZrO}_2$, were neglected.

^b Mass density of H_2O (1.0 g/cm³) and D_2O (1.1 g/cm³) were used for SLD calculation.

in Fig. 6(b). Here the square root of the smeared invariant $\sqrt{Q_{\text{usans}}^{\text{s}}(q)}$ is plotted against D_2O vol% instead of a typical $\sqrt{(d\Omega/d\Sigma)(0)}$. The smeared invariant is defined as, $Q_{\text{usans}}^{\text{s}}(q) = \int_0^{0.001} q[(d\Sigma/d\Omega)(q)]_{\text{usans}}^{\text{s}} dq$, using $((d\Sigma/d\Omega)(q))_{\text{usans}}^{\text{s}}$. The upper limit of $q = 0.001 \text{ \AA}^{-1}$ in the integration was used since USANS scattering of the wet sample in the CM mixture reached the background beyond 0.001 \AA^{-1} . Fig. 6(b) shows that the invariant is a minimum at the CM mixture. When we take negative sign (closed symbol) for $\sqrt{Q_{\text{usans}}^{\text{s}}(q)}$ for both 77% and 100% D_2O (open circles), the data do not lie on a straight line, implying that there is no true match point for the scattering in this q -range.

The presence of residual low q scattering in the CM mixture indicates that there are micron-sized inhomogeneities in the sample. Unfortunately, the CM USANS experiment cannot unambiguously identify the nature of these large scale inhomogeneities. To understand the origin of the micron-sized structure, let us review the Vycor manufacturing process briefly [1]. Alkali-borosilicate glass is melted and quenched. The quenched glass is annealed at a particular temperature depending on the required property. In the annealing process, a bicontinuous phase separation between acid soluble boron-oxide (B_2O_3) and acid insoluble silica (SiO_2) occurs by spinodal decomposition [27] or by nucleation, growth, and rearrangement [28]. The acid soluble B_2O_3 domain is then slowly leached out by hot dilute acid solutions. The leached Vycor is washed using dilute acid and distilled water and then dried. During the annealing process, it is possible that some of the B_2O_3 becomes trapped in isolated domains not accessible by leaching. Incomplete leaching could also leave B_2O_3 – Na_2O or SiO_2 – B_2O_3 – Na_2O [1] domains in Vycor. Residual B_2O_3 domains would prevent complete elimination of scattering contrast in a solution matched to the Vycor matrix. Table 1 shows examples of several contrast conditions. The contrast, $(\Delta \text{SLD})_{\text{CM–B}_2\text{O}_3}^2$, between the CM mixture and amorphous B_2O_3 is $6.72\text{E}+19 \text{ cm}^{-4}$ whereas the contrast between a pore and dry Vycor is $\sim 1.2 \times 10^{21} \text{ cm}^{-4}$. Nevertheless, from the expression relating the scattering invariant to the scattering contrast and volume fraction,

$$\Delta q_v \cdot Q_{\text{usans}}^{\text{s}}(q) = 2\pi^2 \cdot \phi(1 - \phi) \Delta \text{SLD}_{\text{CM–Matrix}}^2, \quad (3)$$

a volume fraction of B_2O_3 of only $\phi \approx 0.6\%$ would be sufficient to produce enough USANS to account for the measured invariant $Q_{\text{usans}}^{\text{s}}(q) \sim 6.72 \times 10^{-5} \text{ cm}^{-1} \text{ \AA}^{-1}$.

4. Conclusion

Strong very low angle scattering with a slope of -2.6 ± 0.2 (corresponding to -3.6 after desmearing) was observed for dry Vycor in the q range of $(3\text{E}-5-1\text{E}-3) \text{ \AA}^{-1}$, below the pore interference peak ($q = 0.023 \text{ \AA}^{-1}$) using USANS. The very low angle scattering could not be contrast matched out completely even with the CM mixture 60/40 $\text{D}_2\text{O}/\text{H}_2\text{O}$ that reduced the pore correlation peak in dry Vycor by three orders of magnitude. The origin of the residual low- q scattering is not known, but isolated regions of B_2O_3 , due to incomplete leaching, are one possibility.

Acknowledgements

We thank Dr. John Barker for providing desmearing program, Dr. Wolfgang K. Haller and Dr. N. Berk for discussion.

References

- [1] T.H. Elmer, Engineering Materials Handbook Ceramics and Glasses, vol. 4, ASM International, Ohio, 1992, pp. 427–432.
- [2] D. Enke, F. Janowski, W. Schwieger, Micropor. Mesopor. Mater. 60 (2003) 19.
- [3] D.W. Schaefer, B.C. Bunker, J.P. Wilcox, Phys. Rev. Lett. 58 (1987) 284.
- [4] P. Wiltzius, F.S. Bates, S.B. Dierker, G.D. Wignall, Phys. Rev. A 36 (1987) 2991.
- [5] P. Levitz, G. Ehret, S.K. Sinha, J.M. Drake, J. Chem. Phys. 95 (8) (1991) 6151.
- [6] M.Y. Lin, S.K. Sinha, J.M. Drake, X.-I. Wu, D.A. Weitz, Phys. Rev. Lett. 71 (1993) 1216.
- [7] F. Formisano, J. Teixeira, J. Phys. – Condens. Matter 12 (2000) A351.
- [8] S.B. Dierker, P. Wiltzius, Phys. Rev. Lett. 66 (1991) 1185.
- [9] J.C. Li, D.K. Ross, L.D. Howe, K.L. Stefanopoulos, J.P.A. Fairclough, R. Heenan, K. Ibel, Phys. Rev. B 49 (1994) 5911.

- [10] A.Ch. Mitropoulos, J.M. Haynes, R.M. Richardson, N.K. Kanellopoulos, *Phys. Rev. B.* 52 (1995) 10035.
- [11] D.P. Bentz, E.J. Garboczi, D.A. Quenard, *Model. Simul. Mater. Sci. Eng.* 6 (1998) 211.
- [12] H.-J. Woo, P.A. Monson, *Phys. Rev. E* 67 (2003) 041207.
- [13] J. Puibasset, R.J.M. Pellenq, *J. Chem. Phys.* 122 (2005) 094704.
- [14] N.F. Berk, *Phys. Rev. Lett.* 58 (1989) 2718.
- [15] N.F. Berk, C.J. Glinka, W. Haller, L.C. Sander, *Mat. Res. Soc. Symp. Proc.* 166 (1990) 409.
- [16] A. Neumann, A. Höhr, P.W. Schmidt, P. Pfeifer, D. Avnir, *Phys. Rev. B.* 38 (2) (1988) 1462.
- [17] J.G. Barker, C.J. Glinka, J.J. Moyer, M.-H. Kim, A.R. Drews, M. Agamalian, *J. Appl. Cryst.* 38 (2005) 1004.
- [18] A.R. Drews, J.G. Barker, C.J. Glinka, M. Agamalian, *Physica B* 241–243 (1998) 189.
- [19] M.-H. Kim, C.J. Glinka, R.N. Carter, *Rev. Sci. Instrum.* 76 (2005) 113904.
- [20] J. Schelten, W. Schmatz, *J. Appl. Cryst.* 13 (1980) 385.
- [21] P. Staron, D. Bellmann, *J. Appl. Cryst.* 35 (2002) 75.
- [22] M.J. Benham, J.C. Cook, J.-C. Li, D.K. Ross, P.L. Hall, B. Sarkissian, *Phys. Rev. B* 39 (1989) 633.
- [23] Unpublished data.
- [24] E.P. Gilbert, L. Auvray, J. Lal, *Macromolecules* 34 (2001) 4942.
- [25] P. Wiltzius, F.S. Bates, S.B. Dierker, G.D. Wignall, *Phys. Rev. A* 36 (1987) 2991.
- [26] J.C. Li, D.K. Ross, L.D. Howe, R. Heenan, K. Ibel, *Phys. Rev. B* 49 (1994) 5911.
- [27] J.W. Chan, *J. Chem. Phys.* 42 (1965) 93.
- [28] W. Haller, *J. Chem. Phys.* 42 (1965) 686.